
1 The relative importance of antecedent soil moisture and precipitation
2 in flood generation in the middle and lower Yangtze River basin

3

4 Sheng Ye¹, Jin Wang¹, Qihua Ran^{2*}, Xiuxiu Chen¹, Lin Liu¹, Jiyu Li¹

5

6 ¹ Institute of Hydrology and Water Resources, School of Civil Engineering, Zhejiang
7 University, Hangzhou 310058, China

8 ² State Key Laboratory of Hydrology-Water Resources and Hydraulic Engineering,
9 Hohai University, Nanjing 210098, China

10

11 * Corresponding author: Qihua Ran

12

13 Email address of the corresponding author: ranqihua@zju.edu.cn

14

15 ~~April~~ July 21, 2022

16

17

18

19 **Abstract**

20 Floods have caused severe environmental and social economic losses worldwide in
21 human history, and are projected to exacerbate due to climate change. Many floods are
22 caused by heavy rainfall with highly saturated soil, however, the relative importance of
23 rainfall and antecedent soil moisture and how it changes from place to place has not
24 been fully understood. Here we examined annual floods from more than 200
25 hydrological stations in the middle and lower Yangtze River basin. Our results indicate
26 that the dominant factor of flood generation shifts from rainfall to antecedent soil
27 moisture with the increase of watershed area. The ratio of the relative importance of
28 antecedent soil moisture and daily rainfall (SPR) is positively correlated with
29 topographic wetness index and has a negative correlation with the magnitude of annual
30 floods. This linkage between watershed characteristics that are easy to measure and the
31 dominant flood generation mechanism provides a framework to quantitatively estimate
32 potential flood risk in ungauged watersheds in the middle and lower Yangtze River
33 basin.

34 **Key words:** flood generation, scaling effect, topographic wetness index

35

36

37 **1. Introduction**

38 Flooding is one of the most destructive and costly natural hazards in the world, resulting
39 in considerable fatalities and property losses (Suresh et al., 2013). River floods have
40 affected nearly 2.5 billion people between 1994 and 2013 worldwide (CRED, 2015),
41 and caused 104 billion dollars losses every year (Desai et al 2015). The damages may
42 be further exacerbated by increasing frequency and intensity of extreme rainfall events
43 according to climate change projections (IPCC 2012; Ohmura and Wild 2002). Flood
44 control infrastructures and more accurate predictions are needed to reduce flood
45 damages, which requires better understanding of the underlying mechanism of flood
46 generation as well as the drivers of change (Villarini & Wasko 2021).

47 Numerous studies have been conducted to investigate the cause of floods across
48 the world (Bloschl et al 2013; Munoz et al 2018; Zhang et al 2018). Many studies
49 focused on examining the environmental and social characteristics that lead to specific
50 catastrophic flood events (Bloschl et al 2013; Liu et al 2020; Zhang et al., 2018). Others
51 concentrated on single locations, usually catchment outlets, to explore the influential
52 factors of floods and the future trends (Brunner et al., 2016; Munoz et al 2018). Yet
53 given the amount of data and time required, it is not practical to apply these detailed
54 studies to hundreds of catchments to generate an overview of the flood generation
55 mechanism at large scale.

56 Recently, researchers started to investigate the dominant flood generation
57 mechanisms at regional scales (Berghuijs et al 2019b; Do et al 2020; Garg & Mishra
58 2019; Smith et al 2018; Trambly et al 2021; Ye et al 2017). Most of these studies are
59 conducted in North America and Europe with well-documented long-term records
60 (Berghuijs et al 2016; Bloschl et al 2019; Do et al 2020; Musselman et al 2018; Rottler

61 et al 2020). ~~Some~~ ~~Some~~ ~~research~~ ~~was~~ ~~was~~ ~~conducted~~ ~~in~~ ~~China~~ ~~recently~~, ~~though~~ ~~is~~ ~~still~~
62 ~~limited~~, ~~and~~ ~~there~~ ~~is~~ ~~a~~ ~~lack~~ ~~of~~ ~~cross~~ ~~scale~~ ~~basin~~ ~~flood~~ ~~research~~. ~~Such~~ ~~researches~~ ~~were~~
63 ~~just~~ ~~conducted~~ ~~in~~ ~~China~~ ~~recently~~, ~~though~~ ~~still~~ ~~limited~~ (Yang et al 2019; Yang et al 2020),
64 ~~though~~ ~~such~~ ~~kind~~ ~~of~~ ~~work~~ ~~is~~ ~~still~~ ~~limited~~, ~~further~~ ~~investigations~~ ~~are~~ ~~needed~~ ~~given~~ ~~the~~
65 ~~considerable~~ ~~spatial~~ ~~heterogeneity~~ ~~and~~ ~~complexity~~ ~~in~~ ~~flood~~ ~~generation~~.

66 As the largest river in China, Yangtze River basin has long suffered from floods. In
67 summer 2020, 378 tributaries of the Yangtze River had floods exceeding the alarm level,
68 causing billions of dollars damage (Xia et al., 2021). With the increasing public
69 awareness, more accurate prediction is needed, which relies on better understanding.
70 However, due to the limitation of observations, there are only a few regional studies of
71 the flood generation mechanism in China, ~~even~~ ~~little~~ ~~with~~ ~~few~~ in the Yangtze River basin
72 (Zhang et al 2018; Yang et al 2019; Yang et al 2020). The large number of dams and
73 reservoirs built along the river further complicated the situation (Feng et al., 2017; Qian
74 et al 2011; Yang et al 2019).

75 Because of the relatively warm temperature, snowmelt has little impact on flood
76 generation in the Yangtze River basin (Yang et al 2020). Floods in the Yangtze River
77 basin usually occur during summer with relatively wet soil and high rainfall (Wang et
78 al 2021). Heavy rainfall with high antecedent soil moisture has also been identified as
79 dominant driver of floods across world (Beighuijs et al 2019b; Garg et al 2019;
80 Trambly et al 2021; Wasko et al 2020). Recently, studies started to examines the
81 relative importance of rainfall and antecedent soil moisture in flood generation
82 (Brunner et al., 2021; Wasko et al., 2021; Bennett et al., 2018; Bertola et al., 2021).
83 Quantitative evaluation of the relative contribution of rainfall and antecedent soil
84 moisture and its change across watersheds is still limited and currently unavailable in

带格式的: 字体颜色: 蓝色

带格式的: 字体颜色: 蓝色

带格式的: 字体颜色: 蓝色

带格式的: 字体颜色: 蓝色

带格式的: 字体颜色: 蓝色

85 China (Liu et al., 2021; Wu et al., 2015).

86 Based on the watersheds in the middle and lower Yangtze River basin, this study
87 attempts to explore the following questions: 1) is there a way to quantitatively describe
88 the relative importance of antecedent soil moisture and rainfall on flood generation; and
89 2) how would this combination of flood-generation rainfall and soil moisture vary
90 across watersheds, and what are the influential factors. Based on the observations and
91 model estimation (Section 2), the spatial distribution patterns of antecedent soil
92 moisture and rainfall were obtained and analyzed to investigate their individual
93 contribution to flood generation and the influential factors ([Section_3](#)). This allows for
94 further examination of the relative importance of antecedent soil moisture and rainfall
95 on flood generation and its linkage to watershed characteristics as well as its
96 implications to flood prediction (Section 4), all the results are summarized in Section 5.

97 **2 Methods**

98 **2.1 Study area**

99 The Yangtze River is the largest river in China, with a total length of 6,300 kilometers
100 and annual discharge of 920km³ at the outlet (Yang et al., 2018). It drains through an
101 area of 1.8*10⁶ km², lying between 90°33'and 122°25'E and 24°30'and 35°45'N, and
102 is home to over 400 million people, most of which live in the middle and lower Yangtze
103 River basin (YZRB) (Cai et al., 2020). The elevation of the YZRB declines from west
104 to east: from over 3000m in Qinghai-Tibet Plateau, to around 1000m in the central
105 mountain region, and the 100m in Eastern China Plain (Wang et al., 2013). The
106 vegetation types in the YZRB are forests, shrubs, grassland and agricultural land,
107 accounting for 11.85%, 12.65%, 32.26% and 42.88% respectively. Grassland and

108 shrubs are the dominant vegetation in the middle and upper YZRB, while the
109 downstream YZRB is dominated by forests and agricultural land (Miao et al., 2010).
110 There are more than 51,000 reservoirs of different sizes in the whole basin, including
111 280 large ones (Peng et al., 2020).

112 Most of the YZRB is semi-humid and humid, with a typical subtropical monsoon
113 climate. The mean annual temperature is approximately 13.0 °C, varying from -4 °C
114 to 18°C downstream. The mean annual precipitation of the whole basin is about 1200
115 mm, increasing from 300mm in the western headwaters to 2400 mm downstream. (Li
116 et al., 2021). Most of the precipitation comes between June and September, the premise
117 of persistent heavy rain in the Yangtze River basin is the frequent activity of weak cold
118 air in the north (Tao et al., 1980) and the intersection of mid-latitude air mass and
119 monsoon air mass (Kato et al., 1985). Studies have found that both annual precipitation
120 and the frequency of extreme precipitation events have increased in the middle and
121 lower reaches of the Yangtze River (Qian et al., 2020; Fu et al., 2013). As a result, floods
122 have occurred frequently in the middle and lower reaches of the Yangtze River, where
123 most of the population in the YZRB live (Liu et al., 2018).

124 **2.2 Data**

125 In this work, we focus on the middle and lower reaches of the Yangtze River for the
126 high population density and increasing flood risk. The 30-meter digital elevation model
127 (DEM) was downloaded from Geospatial Data Cloud (<http://www.gscloud.cn/>), from
128 which the drainage area corresponding to the hydrological station was extracted by
129 ArcGIS. Daily precipitation data and temperature data between 1970 and 2016 from
130 247 meteorological stations within and near the YZRB were downloaded from China
131 Meteorological Data Network (<https://data.cma.cn/>) (Figure 1). The temperature data

132 was used to estimate potential evaporation. The observed precipitation and estimated
133 potential evaporation were interpolated into the whole YZRB using [the](#) Thiessen
134 polygon method (Meena et al., 2013). The interpolated precipitation and potential
135 evaporation were then averaged for the drainage area corresponding to each
136 hydrological station.

137 The daily streamflow data was collected from 267 hydrological stations from
138 Annual Hydrological Report of the People's Republic of China. Among which, 224
139 stations with at least 20 years records from both the period from 1970 to 1990 and the
140 period from 2007 to 2016 were selected. ~~due to confidentiality, we didn't get the data~~
141 ~~from 1990 to 2007 anywhere were not found in online repository.~~ (see Figure S1 for
142 data availability). Information of 361 reservoirs in the middle and lower YZRB,
143 including capacity and controlling area was downloaded and extracted from the Global
144 Reservoir and Dam database (GRanD) (Lehner et al 2011). Previous study showed that
145 this database provides reliable information of middle and large reservoirs in China
146 (Yang et al 2021). Watersheds with more than 80% of the drainage area under control
147 reservoirs according to GRanD database and/or located right downstream of reservoirs
148 and water gates were considered as watersheds under strong regulation (regulated
149 watersheds).

带格式的: 字体颜色: 浅蓝

带格式的: 字体颜色: 浅蓝

150 2.3 Calculation of hydrological and topographic characteristics

151 *Potential evaporation estimation*

152 The temperature data was used to estimate potential evaporation following the
153 Hargreaves method (Allen et al., 1998; Vicente et al., 2014; Berti et al., 2014).

$$154 \quad ET_0 = 0.0023 \times (T_{max} - T_{min})^{0.5} \times (T_{mean} + 17.8) \times Ra \quad (1)$$

155 where ET_0 is potential evaporation (mm/d), T_{max} is the highest temperature ($^{\circ}\text{C}$), T_{min}
156 is the lowest temperature ($^{\circ}\text{C}$), T_{mean} is the mean temperature ($^{\circ}\text{C}$), and Ra is the outer
157 space radiation [$\text{MJ}/(\text{m}^2\cdot\text{d})$], which can be calculated as follows:

$$158 \quad Ra = 37.6 \times d_r \times (\omega_s \sin \varphi \sin \delta + \cos \varphi \cos \delta \sin \omega_s), \quad (2)$$

159 where d_r is the reciprocal of the relative distance between the sun and the earth, ω_s is
160 the angle of sunshine hours, δ is the inclination of the sun (rad), φ is geographic
161 latitude (rad). d_r , δ and ω_s can be calculated by the following formula:

$$162 \quad d_r = 1 + 0.033 \times \cos\left(\frac{2\pi J}{365}\right), \quad (3)$$

$$163 \quad \delta = 0.409 \times \sin\left(\frac{2\pi J}{365} - 1.39\right), \quad (4)$$

$$164 \quad \omega_s = \arcsin(-\tan \varphi \tan \delta), \quad (5)$$

165 where J is the daily ordinal number (January 1st is 1).

166 *Soil water storage estimation*

167 The soil water storage was estimated based on the daily water balance (Berhuijs et al.,
168 2016, 2019):

$$169 \quad \frac{dS}{dt} = P - ET - \max(Q, 0), \quad (6)$$

170 Where S is the soil water storage (mm), which is initially set to 0. Due to the long term
171 of simulation, the change of initial value would not significantly affect the results. P
172 is precipitation (mm/d), Q is discharge normalized by area (mm/d), ET is evaporation
173 (mm/d), which can be calculated from potential evapotranspiration (ET_0), where the

带格式的: 字体颜色: 蓝色

174 soil water storage (S) is used as the upper limit of daily ET:

$$175 \quad ET = \min(0.75 \times ET_0, S), \quad (7)$$

176 The estimation of soil water storage and ET are highly simplified and is not used for
177 prediction but to capture the first order of the seasonal-temporal variation and the
178 relative wetness of soil in the study time period, which ~~and to~~ helps develop a
179 framework that differentiates the relative contribution of precipitation and soil moisture
180 in flood generation.

181 *Topographic wetness index estimation*

182 Topographic wetness index was calculated to represent the combined impacts of
183 drainage area and topographic gradient (Alfonso et al., 2011; Grabs et al., 2009):

$$184 \quad TWI = \ln(A_d/\tan\alpha), \quad (8)$$

185 where A_d is drainage area and α is topographic gradient estimated from DEM. TWI
186 represents the propensity of subsurface flow accumulation and frequency of saturated
187 conditions, thus can be used to predict relative surface wetness and hydrological
188 responses (Meles et al 2020). It is widely used to quantify topographic impact on
189 hydrological processes (i.e., spatial scale effects, hydrological flow path, etc.), as well
190 as in land surface models for hydrological, biogeochemical and ecological processes
191 (Sorensen et al 2006).

192 **2.4 Quantification of the relative importance of soil moisture and precipitation** 193 **during floods**

194 The maximum daily discharge of each year was selected as annual flood, which was
195 then averaged across years as the mean annual maximum flood (AMF). The observed

196 rainfall on that day and the estimated soil water storage at the day before AMF in each
197 year were also averaged across years as daily rainfall (P) and antecedent soil moisture
198 (S_0). Since almost all the AMFs in our study region come during rainy season when
199 rainfall comes in most of the days, it could be difficult to isolate the events of AMFs
200 among consecutive flow events. To avoid the bias that may be caused in event
201 separation, the soil moisture at the day before AMF was used as antecedent soil
202 moisture, instead of the day before the event of AMF. To examine the impacts from
203 long-lasting rainfall event, especially for the large watersheds with longer concentration
204 time, we also calculated the mean accumulated rainfall from two days (rainfall on the
205 flood day and the day before, P_2) to seven days before (weekly rainfall, P_7).

206 The percentile of antecedent soil moisture (S_0) was calculated to represent the
207 relative saturation of soil moisture in the time series; while the percentile of daily
208 rainfall (P) was estimated to show the relative intensity (P'), representing the relative
209 magnitude of rainfall events across time in flood generation. The percentile of
210 accumulated rainfall was also calculated for the two-day to seven-day rainfall.

211 To quantify the relative importance of antecedent soil moisture and rainfall in flood
212 generation, the ratio between these two factors at the AMFs was derived: $SPR = S'/P'$.
213 When SPR is large, the antecedent soil moisture is much closer to the maximum, while
214 the daily rainfall is less extreme, floods are more affected by the antecedent soil
215 moisture. On the other hand, a smaller SPR indicates relatively larger magnitude of
216 rainfall comparing with antecedent soil moisture, that is, rainfall is more extreme and
217 influential in flood generation.

218 **3 Results**

219 3.1 Spatial patterns of antecedent soil moisture and precipitation during floods

220 Figure 2 shows the spatial distribution of the percentile of antecedent soil moisture and
221 daily rainfall during the annual maximum floods (AMFs) in the middle and lower
222 reaches of the Yangtze River. As we can see from Figure 2a, in the middle and lower
223 reaches of YZRB, when AMFs occurred, the percentile of antecedent soil saturation
224 was generally high, most of them are larger than 0.6: the farther away from the main
225 stream, the more saturated the soil was. On the other hand, along and near the main
226 stream and the delta, the antecedent soil saturation rate could be much smaller, even
227 less than 0.4.

228 Figure 2b shows the daily rainfall during the AMFs. As we can see, the percentile
229 of daily rainfall is relatively high (>0.8) at more than half of the study sites, while it is
230 small (<0.5) for the sites along the main stream and in the delta (Figure 2b). Comparison
231 between Figure 2a and b suggests that, except the sites on the main stream and in the
232 delta, sites with relatively high antecedent soil saturation rate (i.e., >0.8 , the blue dots)
233 during AMFs are also the ones with relatively small daily rainfall contribution (i.e.,
234 <0.8 , the light blue and cyan dots). That is, for these sites, the AMFs are usually
235 occurring at a ~~near-saturated soil~~much wetter condition while extreme rainfall at flood
236 day is not necessary, suggesting the relative importance of soil ~~saturation rate~~wetness.
237 For the sites with both the percentile of soil moisture and rainfall between 0.6 and 1,
238 both the antecedent soil moisture and rainfall play important roles in flood generation.
239 As for the sites on the main stream and in the delta, both antecedent soil moisture and
240 rainfall are low during AMFs, this is likely due to the regulations from large reservoirs
241 and water gates.

242 3.2 The scaling effect in the contribution of antecedent soil moisture and rainfall

243 To further investigate the relative importance of antecedent soil moisture and rainfall
244 in flood generation and the potential influential factors, we examined their correlation
245 with catchment area (Figure 3). Given the complicated environmental and social
246 impacts, the regulated watersheds and sites on the main stream are presented separately
247 (the green dots and cyan dots in Figure 3 respectively). Our study will focus on the sites
248 that are not dominated by regulation (the blue dots in Figure 3), for simplicity, we will
249 refer them as natural watersheds.

250 As we can see from Figure 3, during the occurrence of AMFs, the percentile of
251 antecedent soil ~~saturation-wetness~~ increases with watershed area (p -value<0.001),
252 while the percentile of daily rainfall decreases with watershed area (p -value<0.001).
253 That is, with the increase of watershed size, antecedent soil moisture becomes more and
254 more saturated while the precipitation is less and less extreme during AMFs; suggesting
255 the rising contribution of antecedent soil moisture and declining importance of daily
256 precipitation in flood generation. As for the regulated watersheds (green dots in Figure
257 3), there is no clear correlation between drainage area and the percentile of antecedent
258 soil moisture or rainfall, which is understandable. Meanwhile, both the percentile of
259 antecedent soil moisture and rainfall decreases with watershed area for main stream
260 sites.

261 3.3 The scaling impacts on accumulated rainfall

262 The saturation of soil before floods could be due to previous rainfall events, and could
263 also be caused by accumulated rainfall in long-lasting rainfall events that eventually
264 generate floods (Xie et al., 2018). Figure 4 presents the correlation between the
265 percentile of accumulated rainfall and drainage area. When single day rainfall is
266 considered, it is negatively correlated with drainage area (Figure 3a); when

267 accumulated rainfall is considered, the correlation gradually shifts from negative to
268 positive correlation (Figure 4). For example, when two-day rainfall was examined, the
269 correlation between accumulated rainfall and drainage area shifts from negative to
270 positive at 10,000 km²; the negative correlation in Figure 3a is only valid for watersheds
271 larger than 10,000 km² (Figure 4a). This transition area increases from 10,000 km² for
272 two-day rainfall to 100,000 km² for four-day rainfall (Figure 4c). The number of
273 watersheds with negative correlation also decreases. Eventually, the weekly rainfall has
274 similar positive correlation with drainage area like antecedent soil moisture (Figure 4f).
275 The increase of transition area may be explained by the increasing response time and
276 confluence time in large watersheds: it takes days to generate flow events by heavy
277 rainfall and for them to reach outlets where it can be observed in large watersheds. This
278 is also consistent with the conclusion in the Yellow River Basin (Ran et al., 2020) and
279 our previous findings of the dominant flood generation mechanism in the middle and
280 lower YZRB: weekly rainfall is the dominant flood driver for sites on the main streams
281 and the major tributaries (Wang et al 2021). The regulated watersheds don't show
282 significant correlation which is understandable for the strong human intervention. For
283 the negative correlation between accumulated rainfall and drainage area at main stream
284 sites, it is difficult to decide whether it is due to scaling effect or human intervention.

285 **3.4 The interlink of watershed characteristics, flood, antecedent soil moisture and** 286 **rainfall**

287 Figure 5 presents the percentile of antecedent soil moisture and rainfall during the
288 AMFs at the study watersheds, the circles are scaled by watershed size and colored with
289 topographic gradient. Except the watersheds with strong human intervention (regulated
290 ones and the ones on main stream), there is a negative correlation between the

291 contribution of rainfall and antecedent soil moisture. The lower right of the scatter are
292 mostly big blue dots, which are large watersheds with gentle topographic gradient. That
293 is, AMFs usually occur when soil moisture is close to saturation while extreme rainfall
294 is not necessary for AMFs in these watersheds. On top of the scatter are relatively small
295 yellow and green dots, those are medium to small watersheds with steep topographic
296 gradient. That is, AMFs are usually generated with extreme rainfall, while the saturation
297 of soil moisture is not necessary. This negative correlation indicates the shift of
298 dominance in AMFs generation from extreme rainfall to antecedent soil **saturation**
299 **wetness** from small steep watersheds to large flat ones.

300 Figure 6 shows the relative importance of antecedent soil moisture and rainfall. For
301 the natural watersheds (the circles), SPR increases with drainage area and declines with
302 topographic gradient. That is, the larger the drainage area is, the more essential the
303 contribution of antecedent soil moisture to floods is, and the less influential rainfall is
304 in flood generation. For watersheds with similar drainage area (i.e., the green or light
305 blue dots in Figure 6b), topographic gradient also cast impacts on SPR: SPR decreases
306 with slope. That is, the relative importance of rainfall increases at steeper watersheds.
307 This may be attributed to the shortened hydrological response time due to the steep
308 topography which facilitates rainfall induced floods generation. As a combination of
309 both drainage area and topographic gradient, TWI is positively correlated with SPR at
310 natural watersheds, with less scatter than the correlation between SPR and drainage
311 area or topographic gradient alone. That is, watersheds with larger area and gentler
312 topographic gradient that are easier to get wet tend to have larger SPR: soil **saturation**
313 **wetness** is more important in flood generation. There is no significant correlation
314 between SPR and TWI for the regulated watersheds along tributaries (black triangles).
315 However, the sites on main stream show opposite pattern: the SPR at these sites

316 decreases with TWI and drainage area. It is difficult to determine whether this is
317 because of reservoir regulation or not. More data about watersheds larger than
318 10,000km² but with limited human intervention are needed to examine this hypothesis.

319 Besides TWI, SPR is also correlated with the magnitude of AMF (Figure 7). As
320 Figure 7 shows, the area normalized flood peak declines with flood-generation SPR.
321 Watersheds with large flood peak are mostly the ones with steep topographic gradient
322 and small SPR (i.e., SPR<1) and vice versa. Catchments with more extreme floods are
323 the ones with relatively less influence of soil moisture on flood generation. Similar
324 correlation was also found at event scale in our experimental mountainous watershed,
325 which locates at a headwater of Yangtze River (Liu et al 2021).

326 4 Discussion

327 4.1 The relative importance of antecedent soil moisture and rainfall in flood 328 generation

329 While soil moisture and rainfall are the two main drivers of floods in the middle and
330 lower Yangtze River basin, the dominance of each factor varies across the relatively
331 natural watersheds. Floods in large watersheds are usually generated when soil is almost
332 saturated despite of the relatively small rainfall amount, while extreme rainfall is
333 usually observed during floods in small to medium watersheds (blue dots in Figure 3).
334 The rising contribution of antecedent soil moisture in large watersheds was consistent
335 with the findings in Australian watersheds (Wasko & Nathan, 2019); and the declining
336 influence of rainfall at larger watersheds was also found in Indian watersheds (Garg et
337 al 2019). This contrast correlation with watershed size indicates a shift of dominance
338 in AMFs generation, which may be attributed to the longer confluence time in the large

339 watersheds and less heterogeneity in small watersheds.

340 This shift of dominance can be observed more [straightforwardly](#) from the negative
341 correlation between the percentile of rainfall and antecedent soil moisture in Figure 5.
342 The natural watersheds in Figure 5 could be grouped into three classes based on their
343 drainage area and topographic gradient. When a watershed is large and flat, flood
344 occurrence is mainly determined by soil [saturation-wetness](#) (i.e., the big blue dots at the
345 lower right of the scatter); on the other hand, when a watershed is small and steep,
346 heavy rainfall takes over the dominance (i.e., the small yellow and green dots at the
347 upper left of the scatter). Between these two groups are relatively small watersheds with
348 gentle topographic gradient, where the occurrence of AMF requires both highly
349 saturated soil and relatively heavy rainfall. That is, the dominant influential factor(s) in
350 AMFs generation across watersheds is correlated with the topographic characteristics
351 (i.e., watershed size and topographic gradient). This helps quantify the relative
352 importance of soil moisture and rainfall in flood generation in the existing work.

353 This shift of dominance is not observed in the main stream sites (i.e., cyan dots in
354 Figure 3), where the percentile of both antecedent soil moisture and precipitation
355 declines with drainage area. This may be attributed to the more complicated flood
356 generation mechanism at large scale as well as the strong human intervention on main
357 stream (e.g., reservoirs, water gates regulation, etc.) (Gao et al., 2018; Long et al., 2020;
358 Zhang et al., 2017). The major responsibilities of reservoirs on the main stream are to
359 reduce peak flow and postpone the time to flood peak (Volpi et al., 2018). As a result,
360 the original flood peak would be delayed by regulation and the actual flood peak would
361 occur when rainfall declines/stops and soil water drains. Another possibility is that
362 when watershed size is larger than 100,000km², the impact of antecedent soil moisture

363 declines as well. To examine this hypothesis, more data from watersheds larger than
364 100,000km² and with limited human intervention is needed. However, this is above the
365 scope of this work and requires future studies.

366 **4.2 Linkage between topographic characteristics, SPR and floods**

367 The correlation between TWI and SPR (Figure 6c) demonstrates that the relative
368 importance of soil moisture and rainfall could be inferred from topographic
369 characteristics quantitatively. We could derive the relative dominance of soil moisture
370 and rainfall in flood generation in specific watershed from its TWI for the natural
371 watersheds without significant human intervention. Rainfall and soil moisture level
372 have been identified as dominant drivers of floods, individually or together, in
373 watersheds worldwide (Berghuijs et al 2016, 2019b; Garg & Mishra 2019; Trambly et
374 al 2021; Ye et al 2017). Our findings provide a framework to quantify the relative
375 importance of rainfall and soil moisture and to further identify the influential factors of
376 their importance based on topographic characteristics that are easy to measure.

377 Meanwhile, the SPR also present a negative correlation with the magnitude of
378 AMFs (Figure 7). That is, we could infer the mean annual AMF based on SPR for each
379 watershed. Since the characteristic SPR could be estimated from TWI, we could derive
380 quantitative estimation of the mean AMFs from topographic characteristics that are
381 easy to measure, even in watersheds with little hydrologic records.— There is also
382 similar negative correlation between TWI and AMFs (Figure S2). This would be helpful
383 for flood control management in ungauged watersheds, especially in the mountainous
384 watersheds with risks of flash floods. Similar correlation was also found in the
385 observations from our experimental watershed, a headwater of Yangtze River (Liu et al
386 2021). The ratio of observed antecedent soil moisture and event precipitation also

387 presents similar decline trend with discharge at event scale. However, the correlation
388 between SPR and discharge at event scale is preliminary, more data with higher
389 resolution and detailed analysis are needed for validation at event scale. For this study,
390 our goal is to present the framework to derive flood generation SPR that could be
391 estimated from topographic characteristics and to provide information of mean AMFs.

392 In conclusion, based on the topographic characteristics, we could derive the relative
393 importance of soil moisture and rainfall in flood generation (SPR); and from this
394 relative importance ratio, we could further infer the average flood magnitude at these
395 watersheds. As a result, we could link the topographic characteristics and annual floods
396 through the characteristic SPR during the AMFs.

397 **4.3 Implications**

398 Our findings could be helpful for potential flood risk evaluation in ungauged basins,
399 e.g., headwaters in the mountainous region. With the construction of large reservoirs,
400 the capability of flood risk control has improved substantially along [the](#) main stream
401 (Zou et al., 2011; Zhang et al., 2015). However, it is still difficult for quantitative
402 evaluation of flood risk in upstream mountainous watersheds, which are vulnerable to
403 floods but difficult for hydrological modeling and prediction due to little hydrologic
404 records.

405 Our findings suggest that we could derive the flood-generation SPR of each
406 watershed from drainage area and topographic gradient that are easy to measure. The
407 correlation between SPR and flood peak provides information of the mean annual
408 floods in ungauged watersheds. Therefore, in regions without observation data, to build
409 flood control infrastructure such as dams and gates, the mean annual flood peak

410 obtained by SPR based on the topographic characteristics can be used to provide
411 quantitative information for flood control and disaster management. Flood control
412 infrastructures could be designed based on the estimated mean annual flood peak as
413 well as the demographic information. With further validation of this framework at event
414 scale, by using the observed soil moisture from remote sensing data and precipitation
415 forecast to generate real-time prediction of SPR values, we could further provide early
416 warning of floods in these ungauged watersheds. This would be helpful given the
417 increasing possibility of extreme rainfall events due to climate change, But-however,
418 this needs more data and examination are needed in future studies.

419 4.4 Limitations

420 Previous works usually identify the dominant flood generation mechanism based on the
421 comparison of the timing of events (Berghuijs et al 2016; 2019b; Bloschl et al 2017; Ye
422 et al 2017). Similar work has been implemented in our study watersheds, suggesting
423 the importance of soil moisture and rainfall (Wang et al 2021). Based on that, we further
424 looked into the records to quantitatively evaluate the relative importance of soil
425 moisture and rainfall in flood generation. However, there are limitations in our methods.

426 The precipitation data we used were averaged for the study watersheds from 247
427 meteorological stations. Given the large area and considerable spatial heterogeneity, the
428 precipitation data we used may not always be representative of the actual precipitation
429 events. The daily data could also average the rainfall intensity at hourly scale, which
430 could be influential in small mountainous watersheds. ET was scaled as $0.75*ET_0$ to
431 make sure it is smaller than the potential evaporation. This is a simplified estimation of
432 ET; more sophisticated method is needed in further analysis on specific catchments at
433 event scale.

434 The estimation of soil moisture is also highly simplified, which cannot be
435 considered as precise estimation at event scale. To reduce the influence from this
436 simplification, we used the percentile of soil moisture to represent the relative ~~saturation~~
437 ~~wetness~~ of soil moisture as well as the seasonal trend of soil moisture, which was then
438 compared with the percentile of rainfall. While more sophisticated models can be used
439 for soil moisture estimation, there could still be substantial uncertainties ([Zaherpour-et](#)
440 [al., 2018](#); Ran et al 2020). Yet the seasonal trend and the relative magnitude, after
441 averaging through long-term records would be less impacted by the simplification in
442 estimation (Berghuijs et al 2019; Zhang et al 2019).—

443 Our findings may appear different from that in Yang et al (2020), which attributed
444 the dominant flood generation mechanism in the Yangtze River basin to rainfall. This
445 may be explained by different classification criteria: Yang et al (2020) considered both
446 short-rain and long-rain as rainfall impacts while here we only considered the daily
447 rainfall. Thus, the importance of antecedent soil moisture may be considered as long-
448 rain impacts in Yang et al (2020). It is possible that soil moisture at the day before the
449 AMFs may not be the soil moisture before [the](#) event in large catchments due to the long
450 concentration time. We estimated the concentration time for 10 sites with largest
451 drainage area (larger than 100,000 km²): the ones on the main stream and at the outlets
452 of major tributaries following the USBR method (USBR 1973; Gericke & Smithers
453 2014). The concentration time is mostly within two days for main stream sites and is
454 less than 24hr for sites at the outlets of major tributaries (Table S1). Since the rest of
455 the sites are all smaller than these ones, so would be the concentration time. That is, for
456 the natural watersheds we focused on, the concentration time is likely to be within one
457 day. Thus, the soil moisture at the day before AMFs would contribute to the generation
458 of AMFs, and should be applicable for this study.

459 Besides, the exchange with groundwater was not considered in the soil moisture
460 estimation. The exchange with groundwater is more complicated and heterogenous (i.e.,
461 rivers could receive groundwater recharge in hilly area and recharge groundwater in
462 lower land (Che et al 2021)). According to Huang et al. (2021), the variation of
463 groundwater level in the Yangtze River basin is relatively small. Since the goal of this
464 study is to capture the first order seasonal variation of soil moisture and develop a
465 framework that differentiates the relative importance of precipitation and soil moisture
466 in flood generation, in this study, we estimated the soil moisture following Berhuijs (et
467 al 2016, 2019) with a simple water balance equation.

468 Moreover, this work is focused on the relative importance soil moisture and rainfall,
469 the impact of snowmelt is not considered due to the warm and humid climate in the
470 study watersheds. To apply our findings to cold watersheds with significant impact of
471 snow, the snowmelt component needs to be incorporated. In addition, our method is
472 based on the average values from many years. While previous work indicated that the
473 occurrence of floods in our study watersheds are highly concentrated (Wang et al 2021),
474 there could be strong inter-annual variability in other watersheds. In future studies,
475 annual scale and event scale analysis are needed to examine and improve our findings
476 before it can be applied to watersheds with more diverse climate and landscape
477 conditions. There could be uncertainties embedded in the estimation of soil moisture
478 due to the uncertainties in the inputs and model structures. Comprehensive evaluation
479 of the performance and uncertainty is beyond the scope of our study. ~~more~~ More
480 sophisticated comprehensive models with sophisticated groundwater component,
481 remote sensing data, and reanalysis product with higher spatial-temporal resolution are
482 needed to provide more accurate estimation and further validation of soil moisture, ET,
483 and refine the estimation advances our understandings of the flood-generation SPR.

带格式的: 字体颜色: 蓝色

484 **5 Conclusions**

485 Heavy rainfall on highly saturated soil was identified as the dominant flood generation
486 mechanism across world (Berghuijs et al 2019; Wang et al 2021; Wasko et al 2020).
487 This study aims to further evaluate the relative importance of antecedent soil moisture
488 and rainfall on floods generation and the controlling factors. Climate and hydrological
489 data from 224 hydrological stations and 247 meteorological stations in the middle and
490 lower reaches of the Yangtze River basin was analyzed, along with the modeled soil
491 moisture. Except the regulated watersheds, the relative importance of antecedent soil
492 moisture and daily rainfall present significant correlation with drainage area: the larger
493 the watershed is, the more essential antecedent soil saturation rate is in flood generation,
494 the less important daily rainfall is.

495 Using the percentile of antecedent soil moisture and rainfall as coordinates, the
496 flood generation mechanism(s) of study watersheds could be grouped into three classes:
497 antecedent soil moisture dominated large flat watersheds, heavy rainfall dominated
498 steep and small to middle size watersheds, and small to middle size watersheds with
499 gentle topographic gradient where floods occurrence requires both highly saturated soil
500 and heavy rainfall. Our analysis further shows that the ratio of relative importance
501 between antecedent soil moisture and rainfall (SPR) can be predicted by topographic
502 wetness index. When the topographic wetness index is large, the dominance of
503 antecedent soil moisture for extreme floods is stronger, and *vice versa*. The SPR also
504 presents negative correlation with area normalized flood peak.

505 With the potential increase of extreme rainfall events (Gao et al., 2016; Chen et
506 al., 2016), upstream mountainous watersheds in the middle and lower Yangtze River
507 basin are facing higher risk of extreme floods. The lack of hydrological records further

508 increases the vulnerability of people in these watersheds. The flood risks could be
509 reduced by construction of flood control facilities, but it is difficult to set flood control
510 standards in these ungauged watersheds. Our findings provide a framework to
511 quantitatively estimate the possible flood risk for these ungauged watersheds. Based on
512 measurable watershed characteristics (i.e., drainage area and topographic gradient), the
513 flood generation SPR could be derived, which could then be used to estimate the mean
514 annual flood. This information can provide scientific support for flood control
515 management as well as infrastructures construction.

516 Future analysis at event scale could help generate the flood-generation curve
517 between SPR and discharge at event scale to further improve flood risk predictions in
518 these small ungauged watersheds. With more data from other regions and improved
519 estimation or observation of soil moisture, we could expand our analysis to watersheds
520 with more diverse climate and topographic characteristics to examine and refine our
521 findings and to enhance our understandings of flood generation. Comparison between
522 different time periods (i.e., before and after 2000) could also reveal temporal changes
523 in floods generation, which may be linked to the climate change, yet longer data records
524 are needed to generation representative patterns.

525

526 **Data availability**

527 DEM data was downloaded from Geospatial Data Cloud at <http://www.gscloud.cn/>.
528 Climatological data used in this study was obtained from China Meteorological Data
529 Network, which can be accessed at <http://data.cma.cn/>. Discharge data comes from
530 Annual Hydrological Report of the People's Republic of China issued by Yangtze River
531 Water Resources Commission.

532

533 **Acknowledgements**

534 This research was funded by the National Key Research and Development Program of
535 China (2019YFC1510701-01), and National Natural Science Foundation of China
536 (51979243).

537

538 **References**

539 Abbas, S.A., Xuan, Y. and Song, X.: Quantile Regression Based Methods for
540 Investigating Rainfall Trends Associated with Flooding and Drought Conditions.
541 Water Resources Management, 33(12), 4249-4264, [https://doi:10.1007/s11269-](https://doi:10.1007/s11269-019-02362-0)
542 019-02362-0, 2019.

543 Alfonso R., Nilza M. R.C., and Anderson L. R.: Numerical Modelling of the
544 Topographic Wetness Index: An Analysis at Different Scales, International
545 Journal of Geosciences(4), 476-483, <https://doi:10.4236/ijg.2011.24050>, 2011.

546 Allen R. G., Pereira L. S. and Raes D.: Crop evapotranspiration-Guidelines for
547 computing crop water requirements FAO Irrigation and drainage paper
548 NO.56(Electric Publication)[M], Rome , Italy:FAO, 1998.

549 Bennett, B., Leonard, M., Deng, Y., Westra, S.: An empirical investigation into the
550 effect of antecedent precipitation on flood volume. J. Hydrol. 567, 435–445.
551 <https://doi.org/10.1016/j.jhydrol.2018.10.025>, 2018.

552 Berghuijs, W.R., Allen, S.T., Harrigan, S. and Kirchner, J.W.: Growing Spatial Scales
553 of Synchronous River Flooding in Europe. Geophysical Research Letters, 46(3),
554 1423-1428, <https://doi:10.1029/2018GL081883>, 2019a.

555 Berghuijs, W.R., Harrigan, S., Molnar, P., Slater, L.J. and Kirchner, J.W.: The Relative
556 Importance of Different Flood-Generating Mechanisms Across Europe. Water
557 Resources Research, 55(6), 4582-4593, <https://doi:10.1029/2019WR024841>,
558 2019b.

559 Berghuijs, W.R., Woods, R.A., Hutton, C.J. and Sivapalan, M.: Dominant flood
560 generating mechanisms across the United States. Geophysical Research Letters,
561 43(9), 4382-4390, <https://doi:10.1002/2016GL068070>, 2016.

562 Bertola, M., Viglione, A., Vorogushyn, S., Lun, D., Merz, B., Blöschl, G.: Do small
563 and large floods have the same drivers of change? A regional attribution analysis
564 in Europe. Hydrol. Earth Syst. Sci. 25, 1347–1364. [https://doi.org/10.5194/hess-](https://doi.org/10.5194/hess-25-1347-2021)
565 25-1347-2021, 2021.

-
- 566 Bloschl, G., Nester, T., Komma, J., Parajka, J. and Perdigao, R.A.P.: The June 2013
567 flood in the Upper Danube Basin, and comparisons with the 2002, 1954, and 1899
568 floods. *Hydrol. Earth Syst. Sci.*, 17, 5197–5212, 2013.
- 569 Blöschl, G., Hall, J., Parajka, J., Perdigão, R. A., Merz, B., Arheimer, B., et al.:
570 Changing climate shifts timing of European floods. *Science*, 357(6351), 588–
571 590. <https://doi.org/10.1126/science.aan2506>, 2017.
- 572 Bloschl, G., Hall, J., Viglione, A., Perdigao, R.A., Parajka, J., Merz, B., et al.: Changing
573 climate both increases and decreases European river floods, *Nature*, 573, 108 –
574 111, 2019.
- 575 Berti, A., Tardivo, G., Chiaudani, A., Rech, F. and Borin, M.: Assessing reference
576 evapotranspiration by the Hargreaves method in north-eastern Italy. *Agricultural
577 Water Management*, 140, 20-25, <https://doi:10.1016/j.agwat.2014.03.015>, 2014.
- 578 Brunner, M. I., Seibert, J. and Favre, A.C.: Bivariate return periods and their importance
579 for flood peak and volume estimation. *Wire's Water*, 3, 819 – 833.
580 <https://doi.org/10.1002/wat2.1173>, 2016.
- 581 Brunner, M. I., Gilleland, E., Wood, A., Swain, D. L., and Clark, M.: Spatial
582 dependence of floods shaped by spatiotemporal variations in meteorological and
583 land - surface processes. *Geophysical Research Letters*, 47, e2020GL088000.
584 <https://doi.org/10.1029/2020GL088000>, 2020.
- 585 Brunner, M. I., Swain, D. L., Wood, R.R. et al. An extremeness threshold determines
586 the regional response of floods to changes in rainfall extremes. *Commun Earth
587 Environ* 2, 173. <https://doi.org/10.1038/s43247-021-00248-x>, 2021.
- 588 Cai, Q. H.: Great protection of Yangtze River and watershed ecology, *Yangtze River
589 (01)*, 70-74, <https://doi:10.16232/j.cnki.1001-4179.2020.01.011>, 2020.
- 590 Cen, S.-x., Gong, Y.-f., Lai, X. and Peng, L.: The Relationship between the
591 Atmospheric Heating Source/Sink Anomalies of Asian Monsoon and

592 Flood/Drought in the Yangtze River Basin in the Meiyu Period. *Journal of*
593 *Tropical Meteorology*, 21(4), 352-360, 2015.

594 Che, Q., Su, X., Zheng, S., Li, Y.: Interaction between surface water and groundwater
595 in the Alluvial Plain (anqing section) of the lower Yangtze River Basin:
596 environmental isotope evidence. *Journal of Radioanalytical and Nuclear*
597 *Chemistry*, 329, 1331–1343, 2021.

598 Chen, Y. and Zhai, P.: Mechanisms for concurrent low-latitude circulation anomalies
599 responsible for persistent extreme precipitation in the Yangtze River Valley.
600 *Climate Dynamics*, 47(3-4), 989-1006, <https://doi:10.1007/s00382-015-2885-6>,
601 2016.

602 CRED (2015). The human cost of natural disasters: A global perspective: Centre for
603 research on the epidemiology of disasters.

604 Deb, P., Kiem, A.S. and Willgoose, G.: Mechanisms influencing non-stationarity in
605 rainfall-runoff relationships in southeast Australia. *Journal of Hydrology*, 571,
606 749-764, <https://doi:10.1016/j.jhydrol.2019.02.025>, 2019.

607 Desai, B., Maskrey, A., Peduzzi, P., De Bono, A., & Herold, C. Making Development
608 Sustainable: The Future of Disaster Risk Management. Global Assessment Report
609 on Disaster Risk Reduction <http://archive-ouverte.unige.ch/unige:78299> (UNISDR,
610 2015).

611 Do, H. X., Mei, Y., & Gronewold, A. D.: To what extent are changes in flood magnitude
612 related to changes in precipitation extremes? *Geophysical Research Letters*, 47,
613 e2020GL088684. <https://doi.org/10.1029/2020GL088684>, 2020.

614 Fang, X. and Pomeroy, J.W.: Impact of antecedent conditions on simulations of a flood
615 in a mountain headwater basin. *Hydrological Processes*, 30(16), 2754-2772,
616 <https://doi:10.1002/hyp.10910>, 2016.

617 Feng, B. F., Dai M. L. and Zhang T.: Effect of Reservoir Group Joint Operation on
618 Flood Control in the Middle and Lower Reaches of Yangtze River, *Journal of*
619 *Water Resources Research* (3), 278-284, <https://doi:10.12677/JWRR.2017.63033>,
620 2017.

621 Fu, G., Yu, J., Yu, X., Ouyang, R., Zhang, Y., Wang, P., Liu, W. and Min, L.: Temporal
622 variation of extreme rainfall events in China, 1961-2009. *Journal of Hydrology*,
623 487, 48-59, <https://doi:10.1016/j.jhydrol.2013.02.021>, 2013.

624 Gao, T. and Xie, L.: Spatiotemporal changes in precipitation extremes over Yangtze
625 River basin, China, considering the rainfall shift in the late 1970s. *Global and*
626 *Planetary Change*, 147, 106-124, <https://doi:10.1016/j.gloplacha.2016.10.016>,
627 2016.

628 Gao, Y., Wang, H., Lu, X., Xu, Y., Zhang, Z. and Schmidt, A.R.: Hydrologic Impact
629 of Urbanization on Catchment and River System Downstream from Taihu Lake.
630 *Journal of Coastal Research*, 82-88, <https://doi:10.2112/SI84-012.1>, 2018.

631 Garg, S., & Mishra, V.: Role of extreme precipitation and initial hydrologic conditions
632 on floods in Godavari river basin, India. *Water Resources Research*, 55, 9191–
633 9210. <https://doi.org/10.1029/2019WR025863>, 2019.

634 Grabs, T., Seibert, J., Bishop, K. and Laudon, H.: Modeling spatial patterns of saturated
635 areas: A comparison of the topographic wetness index and a dynamic distributed
636 model. *Journal of Hydrology*, 373(1-2), 15-23,
637 <https://doi:10.1016/j.jhydrol.2009.03.031>, 2009.

638 Huang, C., Zhou, Y., Zhang, S., Wang, J., Liu, F., Gong, C., Yi, C., Li, L., Zhou, H.,
639 Wei, L., Pan, X., Shao, C., Li, Y., Han, W., Yin, Z., and Li, X.: Groundwater
640 resources in the Yangtze River Basin and its current development and utilization[J].
641 *Geology of China*, 2021, 48(4):979-1000.

642 IPCC. *Managing the Risks of Extreme Events and Disasters to Advance Climate*
643 *Change Adaptation* (eds Field, C. B. et al.) (Cambridge Univ. Press, 2012).

644 Kato, K.: On the Abrupt Change in the Structure of the Baiu Front over the China
645 Continent in Late May of 1979. *Journal of the Meteorological Society of Japan*,
646 63(1), 20-36, https://doi:10.2151/jmsj1965.63.1_20, 1985.

647 Kazuki, T., Oliver C. S. V., Masahiro, R.: Spatial variability of precipitation and soil
648 moisture on the 2011 flood at chao phraya river basin. *International Water*
649 *Technology Association, Proceedings of Hydrology and Water Resources*, B, 17-
650 21, 2013.

651 Kemter, M., Merz, B., Marwan, N., Vorogushyn, S., & Blöschl, G.: Joint trends in flood
652 magnitudes and spatial extents across Europe. *Geophysical Research Letters*, 47,
653 e2020GL087464. <https://doi.org/10.1029/2020GL087464>, 2020.

654 Lehner, B., C. Reidy Liermann, C. Revenga, C. Vörösmarty, B. Fekete, P. Crouzet, P.
655 Döll, M. Endejan, K. Frenken, J. Magome, C. Nilsson, J.C. Robertson, R. Rodel,
656 N. Sindorf, and D. Wisser. 2011. High-resolution mapping of the world's

657 reservoirs and dams for sustainable river-flow management. *Frontiers in Ecology*
658 *and the Environment* 9 (9): 494-502.

659 Li, Q., Wei, F. and Li, D.: Interdecadal variation of East Asian summer monsoon and
660 drought/flood distribution over eastern China in the last 159 years. *Journal of*
661 *Geographical Sciences*, 21(4), 579-593, <https://doi:10.1007/s11442-011-0865-2>,
662 2011.

663 Li, X., Zhang, K., Gu, P., Feng, H., Yin, Y., Chen, W. and Cheng, B.: Changes in
664 precipitation extremes in the Yangtze River Basin during 1960-2019 and the
665 association with global warming, ENSO, and local effects. *Science of the Total*
666 *Environment*, 760, <https://doi:10.1016/j.scitotenv.2020.144244>, 2021.

667 Liu, B., Yan, Y., Zhu, C., Ma, S., & Li, J.: Record-breaking Meiyu rainfall around the
668 Yangtze River in 2020 regulated by the subseasonal phase transition of the North
669 Atlantic Oscillation. *Geophysical Research Letters*, 47, e2020GL090342.
670 <https://doi.Org/10.1029/2020GL090342>, 2020.

671 Liu, L., Ye, S., Chen, C., Pan, H. and Ran, Q.: Nonsequential Response in Mountainous
672 Areas of Southwest China. *Frontiers in Earth Science*, 9: 1-15. doi:
673 10.3389/feart.2021.660244, 2021

674 Liu, N., Jin, Y. and Dai, J.: Variation of Temperature and Precipitation in Urban
675 Agglomeration and Prevention Suggestion of Waterlogging in Middle and Lower
676 Reaches of Yangtze River. 3rd International Conference on Energy Equipment
677 Science and Engineering (Iceese 2017), 128, [https://doi:10.1088/1755-](https://doi:10.1088/1755-1315/128/1/012165)
678 [1315/128/1/012165](https://doi:10.1088/1755-1315/128/1/012165), 2018.

679 Liu, S., Huang, S., Xie, Y., Wang, H., Leng, G., Huang, Q., Wei, X., and Wang, L.:
680 Identification of the Non-stationarity of Floods: Changing Patterns, Causes, and
681 Implications, *Water Resour. Manag.*, 33, 939–953, 2018.

682 Liu, Y., Xinyu, L., Liancheng, Z., Yang, L., Chunrong, J., Ni, W. and Juan, Z.:
683 Quantifying rain, snow and glacier meltwater in river discharge during flood
684 events in the Manas River Basin, China. *Natural Hazards*, 108(1), 1137-1158,
685 <https://doi:10.1007/s11069-021-04723-8>, 2021.

686 Long, L.H., Ji, D.B., Yang, Z.Y., Cheng, H.Q., Yang, Z.J., Liu, D.F., Liu, L. and Lorke,
687 A.: Tributary oscillations generated by diurnal discharge regulation in Three
688 Gorges Reservoir. *Environmental Research Letters*, 15(8),
689 <https://doi:10.1088/1748-9326/ab8d80>, 2020.

690 Lu, M., Wu, S.-J., Chen, J., Chen, C., Wen, Z. and Huang, Y.: Changes in extreme
691 precipitation in the Yangtze River basin and its association with global mean
692 temperature and ENSO. *International Journal of Climatology*, 38(4), 1989-2005,
693 <https://doi:10.1002/joc.5311>, 2018.

694 Meles, M.B., Younger, S.E., Jackson, C.R., Du, E., Drover, D.: Wetness index based
695 on landscape position and topography (WILT): Modifying TWI to reflect
696 landscape position, *Journal of Environmental Management* 255, 109863, 2020.

697 Miao, Q., Huang, M. and Li, R., Q.: Response of net primary productivity of vegetation
698 in Yangtze River Basin to future climate change. *Journal of Natural Resources*, 25,
699 08(2010):1296-1305, doi:CNKI:SUN:ZRZX.0.2010-08-007, 2015.

700 Munoz, S.E., Giosan, L., Therrell, M.D., Remo, J.W.F., Shen, Z., Sullivan, R.M.,
701 Wiman, C., O'Donnell, M., and Donnelly, J.P.: Climatic control of Mississippi
702 River flood hazard amplified by river engineering, 556, 95 – 98, 2018.

703 Musselman, K.N., Lehner, F., Ikeda, K., Clark, M.P., Prein, A.F., Liu, C., Barlage, M.
704 and Rasmussen, R.: Projected increases and shifts in rain-on-snow flood risk over
705 western North America, *Nature Climate Change*, 8, 808 – 812, 2018.

706 Ockert J. G. and Jeff C. S.: Review of methods used to estimate catchment response
707 time for the purpose of peak discharge estimation, *Hydrological Sciences Journal*,
708 59:11, 1935-1971, DOI: 10.1080/02626667.2013.866712, 2014.

709 Ohmura, A. and Wild, M.: Is the hydrological cycle accelerating? *Science*, 298, 1345–
710 1346, 2002.

711 Pegram, G. and Bardossy, A.: Downscaling Regional Circulation Model rainfall to
712 gauge sites using recorelation and circulation pattern dependent quantile-quantile
713 transforms for quantifying climate change. *Journal of Hydrology*, 504, 142-159,
714 <https://doi:10.1016/j.jhydrol.2013.09.014>, 2013.

715 Peng, T., Tian, H., Singh, V. P., Chen, M., Liu, J., Ma, H. B. and Wang, J. B.:
716 Quantitative assessment of drivers of sediment load reduction in the Yangtze River
717 basin, China, *Journal of Hydrology*, 580,
718 <https://doi:10.1016/j.jhydrol.2019.124242>, 2020.

719 Qian, H. and Xu, S.-B.: Prediction of Autumn Precipitation over the Middle and Lower
720 Reaches of the Yangtze River Basin Based on Climate Indices. *Climate*, 8(4),
721 <https://doi:10.3390/cli8040053>, 2020.

722 Ran, Q., Chen, X., Hong Y., Ye S., and Gao J.: Impacts of terracing on hydrological
723 processes: A case study from the Loess Plateau of China. *Journal of Hydrology*,
724 588, <https://doi.org/10.1016/j.jhydrol.2020.125045>, 2020.

725 Ran, Q., Zong, X., Ye, S., Gao, J. and Hong, Y.: Dominant mechanism for annual
726 maximum flood and sediment events generation in the Yellow River basin. *Catena*,
727 187, <https://doi.org/10.1016/j.catena.2019.104376>, 2020.

728 Ray S. M., Ramakar J. and Kishanjit K. K.: Precipitation-runoff simulation for a
729 Himalayan River Basin, India using artificial neural network algorithms, *Sciences*
730 *in Cold and Arid Regions*, 5(1), 85-95, 2013.

731 Rottler, E., Francke, T., Burger, G., and Bronstert, A.: Long-term changes in central
732 European river discharge for 1869–2016: impact of changing snow covers,
733 reservoir constructions and an intensified hydrological cycle, *Hydrol. Earth Syst.*
734 *Sci.*, 24, 1721–1740, 2020.

735 Smith, J. A., Cox, A. A., Baeck, M. L., Yang, L., and Bates, P.: Strange floods: the
736 upper tail of flood peaks in the United States, *Water Resour. Res.*, 54, 6510–6542,
737 2018.

738 Sorensen, R., Zinko, U., and Seibert, J.: On the calculation of the topographic wetness
739 index: evaluation of different methods based on field observations, *Hydrology and*
740 *Earth System Sciences*, 10, 101–112, 2006.

741 Su, Z., Ho, M., Hao, Z., Lall, U., Sun, X., Chen, X. and Yan, L.: The impact of the
742 Three Gorges Dam on summer streamflow in the Yangtze River Basin.
743 *Hydrological Processes*, 34(3), 705-717, <https://doi.org/10.1002/hyp.13619>, 2020.

744 Suresh, S. S., Benefit O., Augustine T., and Trevor P. : Peoples' Perception on the
745 Effects of Floods in the Riverine Areas of Ogbia Local Government Area of
746 Bayelsa State, Nigeria, *Knowledge Management*, [https://doi.org/10.18848/2327-](https://doi.org/10.18848/2327-7998/CGP/v12i02/50793)
747 [7998/CGP/v12i02/50793](https://doi.org/10.18848/2327-7998/CGP/v12i02/50793), 2013.

748 Tao, S. Y., *Rainstorm in China [M]*, Beijing: Science Press, 1980.(in Chinese)

749 Trambly, Y., Villarini, G., El Khalki, E. M., Gründemann, G., & Hughes, D.:
750 Evaluation of the drivers responsible for flooding in Africa. *Water Resources*
751 *Research*, 57, e2021WR029595. <https://doi.org/10.1029/2021WR029595>, 2021.

752 USBR (United States Bureau of Reclamation), 1973. Design of small dams. 2nd ed.
753 Washington, DC: Water Resources Technical Publications.

754 Vicente-Serrano, S.M., Azorin-Molina, C., Sanchez-Lorenzo, A., Revuelto, J., Lopez-
755 Moreno, J.I., Gonzalez-Hidalgo, J.C., Moran-Tejeda, E. and Espejo, F.: Reference
756 evapotranspiration variability and trends in Spain, 1961-2011. *Global and*
757 *Planetary Change*, 121, 26-40, <https://doi:10.1016/j.gloplacha.2014.06.005>, 2014.

758 Volpi, E., Di Lazzaro, M., Bertola, M., Viglione, A. and Fiori, A.: Reservoir Effects on
759 Flood Peak Discharge at the Catchment Scale. *Water Resources Research*, 54(11),
760 9623-9636, <https://doi:10.1029/2018wr023866>, 2018.

761 Wang, H., Zhou, Y., Pang, Y. and Wang, X.: Fluctuation of Cadmium Load on a Tide-
762 Influenced Waterfront Lake in the Middle-Lower Reaches of the Yangtze River.
763 *Clean-Soil Air Water*, 42(10), 1402-1408, <https://doi:10.1002/clen.201300693>,
764 2014.

765 Wang, J., Ran, Q., Liu, L., Pan, H. and Ye, S.: Study on the Dominant Mechanism of
766 Extreme Flow Events in the Middle and Lower Reaches of the Yangtze River,
767 *China Rural Water and Hydropower*, Accepted.

768 Wang, R., Yao, Z., Liu, Z., Wu, S., Jiang, L. and Wang, L.: Snow cover variability and
769 snowmelt in a high-altitude ungauged catchment. *Hydrological Processes*, 29(17),
770 3665-3676, <https://doi:10.1002/hyp.10472>, 2015.

771 Wang, W., Xing W., Yang, T., Shao, Q., Peng, S., Yu, Z., and Yong, B.: Characterizing
772 the changing behaviours of precipitation concentration in the Yangtze River Basin,
773 China. *Hydrological Processes*, 27(24), 3375-3393, <https://doi:10.1002/hyp.9430>,
774 2013.

775 Wang, Z. and Plate, E.: Recent flood disasters in China. *Proceedings of the Institution*
776 *of Civil Engineers – Water and Maritime Engineering* (3),
777 <https://doi:10.1680/wame.2002.154.3.177>, 2002.

778 Wasko, C. and Nathan, R.: Influence of changes in rainfall and soil moisture on trends
779 in flooding. *Journal of Hydrology*, 575, 432-441,
780 <https://doi:10.1016/j.jhydrol.2019.05.054>, 2019.

781 Wasko, C., Nathan, R., & Peel, M. C.: Changes in antecedent soil moisture modulate
782 flood seasonality in a changing climate. *Water Resources Research*, 56,
783 e2019WR026300. <https://doi.org/10.1029/2019WR026300>, 2020.

784 Wasko, C., Nathan, R., Stein, L., O'Shea, D.: Evidence of shorter more extreme
785 rainfalls and increased flood variability under climate change. *J. Hydrol.* 603,
786 126994. <https://doi.org/10.1016/j.jhydrol.2021.126994>, 2021.

787 Wu, X. S., Guo, S. L. and Ba, H. H.: Long-term precipitation forecast method based on
788 SST multipole index, *Journal of water conservancy*(10), 1276-1283,
789 <https://doi:10.13243/j.cnki.slx.20180544>, 2018.

790 Xia, J. and Chen, J.: A new era of flood control strategies from the perspective of
791 managing the 2020 Yangtze River flood. *Science China-Earth Sciences*, 64(1), 1-
792 9, <https://doi:10.1007/s11430-020-9699-8>, 2021.

793 Xie, Z., Du, Y., Zeng, Y. and Miao, Q.: Classification of yearly extreme precipitation
794 events and associated flood risk in the Yangtze-Huaihe River Valley. *Science*
795 *China-Earth Sciences*, 61(9), 1341-1356, <https://doi:10.1007/s11430-017-9212-8>,
796 2018.

797 Yang, H.F., Yang, S.L., Xu, K.H., Milliman, J.D., Wang, H., Yang, Z., Chen, Z. and
798 Zhang, C.Y.: Human impacts on sediment in the Yangtze River: A review and new
799 perspectives. *Global and Planetary Change*, 162, 8-17,
800 <https://doi:10.1016/j.gloplacha.2018.01.001>, 2018.

801 Yang, L., Wang, L., Li, X. and Gao, J.: On the flood peak distributions over China.
802 *Hydrology and Earth System Sciences*, 23(12), 5133-5149,
803 <https://doi:10.5194/hess-23-5133-2019>, 2019.

804 Yang, W., Yang, H., and Yang, D.: Classifying floods by quantifying driver
805 contributions in the Eastern Monsoon Region of China, *Journal of Hydrology*, 585,
806 124767, 2020.

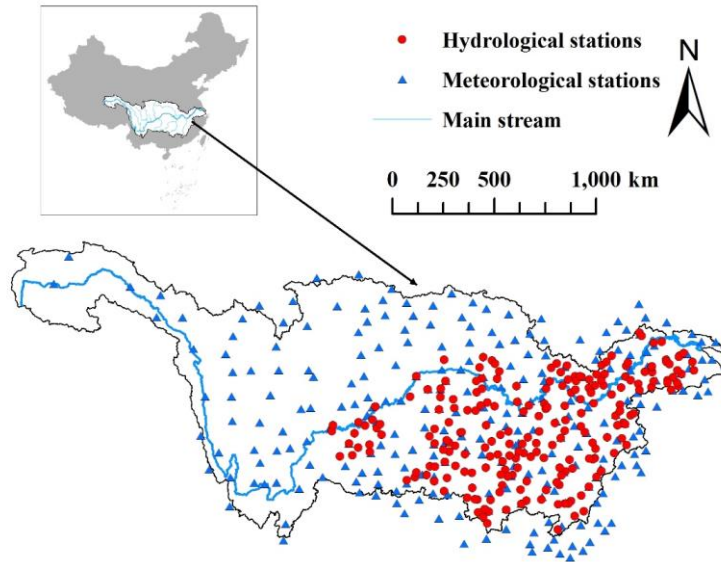
807 Yang, W., Yang, H., Yang, D., and Hou, A.: Causal effects of dams and land cover
808 changes on flood changes in mainland China. *Hydrol. Earth Syst. Sci.*, 25, 2705–
809 2720, 2021.

810 Ye, S., Li, H., Leung, L.R., Guo, J., Ran, Q., Demissie, Y., et al., 2017. Understanding
811 flood seasonality and its temporal shifts within the contiguous United States. *J.*
812 *Hydrometeorol.* 18 (7), 1997–2009.

813 Ye, X., Xu, C.-Y., Li, Y., Li, X. and Zhang, Q.: Change of annual extreme water levels
814 and correlation with river discharges in the middle-lower Yangtze River:
815 Characteristics and possible affecting factors. *Chinese Geographical*
816 *Science*, 27(2), 325-336, <https://doi:10.1007/s11769-017-0866-x>, 2017.

-
- 817 Yu, F., Chen, Z., Ren, X. and Yang, G.: Analysis of historical floods on the Yangtze
818 River, China: Characteristics and explanations. *Geomorphology*,113(3-4), 210-
819 216, <https://doi:10.1016/j.geomorph.2009.03.008>, 2009.
- 820 ~~Zaherpour, J., Gosling, S. N., Mount, N., Schmied, H. M., Veldkamp, T. I., et~~
821 ~~al.:Worldwide evaluation of mean and extreme runoff from six global-scale~~
822 ~~hydrological models that account for human impacts. *Environmental Research*~~
823 ~~*Letters*, 13(6), 065015. <https://doi.org/10.1088/1748-9326/aac547>, 2018.~~
- 824 Zhang, H., Liu, S., Ye, J. and Yeh, P.J.F.: Model simulations of potential contribution
825 of the proposed Huangpu Gate to flood control in the Lake Taihu basin of China.
826 *Hydrology and Earth System Sciences*, 21(10), 5339-5355,
827 <https://doi:10.5194/hess-21-5339-2017>, 2017.
- 828 Zhao, J., Li, J., Yan, H., Zheng, L. and Dai, Z.: Analysis on the Water Exchange
829 between the Main Stream of the Yangtze River and the Poyang Lake. 2011 3rd
830 International Conference on Environmental Science and Information Application
831 Technology Esiat 2011, Vol 10, Pt C,10, 2256-2264,
832 <https://doi:10.1016/j.proenv.2011.09.353>, 2011.
- 833 Zhang, S., Kang, L. and He, X.: Equal proportion flood retention strategy for the leading
834 multireservoir system in upper Yangtze River. *International Conference on Water*
835 *Resources and Environment, WRE 2015*, 2015.
- 836 Zhang, W., Villarini, G., Vecchi, G.A. and Smith, J. A.: Urbanization exacerbated the
837 rainfall and flooding caused by hurricane Harvey in Houston. *Nature*, 563, 384 –
838 388, 2018.
- 839 Zhang, K., Wang, Q., Chao, L., Ye, J., Li, Z., Yu, Z., Yang, T. and Ju, Q.: Ground
840 observation-based analysis of soil moisture spatiotemporal variability across a
841 humid to semi-humid transitional zone in China. *Journal of Hydrology*, 574, 903-
842 914, 2019.
- 843 Zou, B., Li, Y., Feng, B.: Analysis on dispatching influence of Three Gorges Reservoir
844 on water level of main stream in mid-lower reaches of Yangtze River: a case study
845 of flood in July,2010. *Yangtze River*, 42.06:80-82+100. doi:10.16232/j.cnki.1001-
846 4179.2011.06.004, 2011.

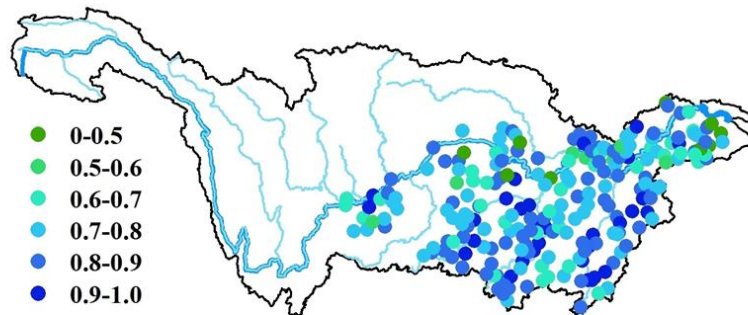
847
848



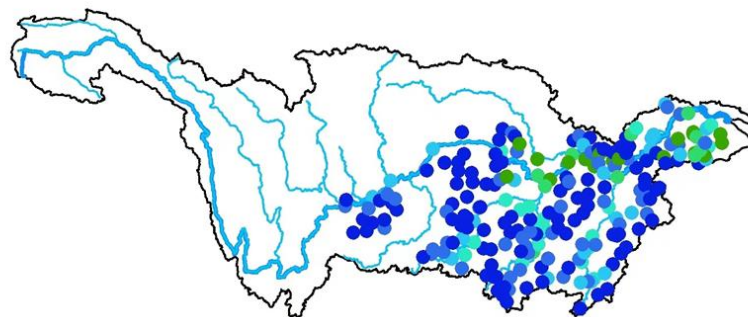
849

850 **Figure 1:** Map of the Yangtze River basin, and the meteorological stations and
851 hydrological stations. The blue line is the main stream of Yangtze River.

852



(a) Percentile of antecedent soil moisture



(b) Percentile of precipitation

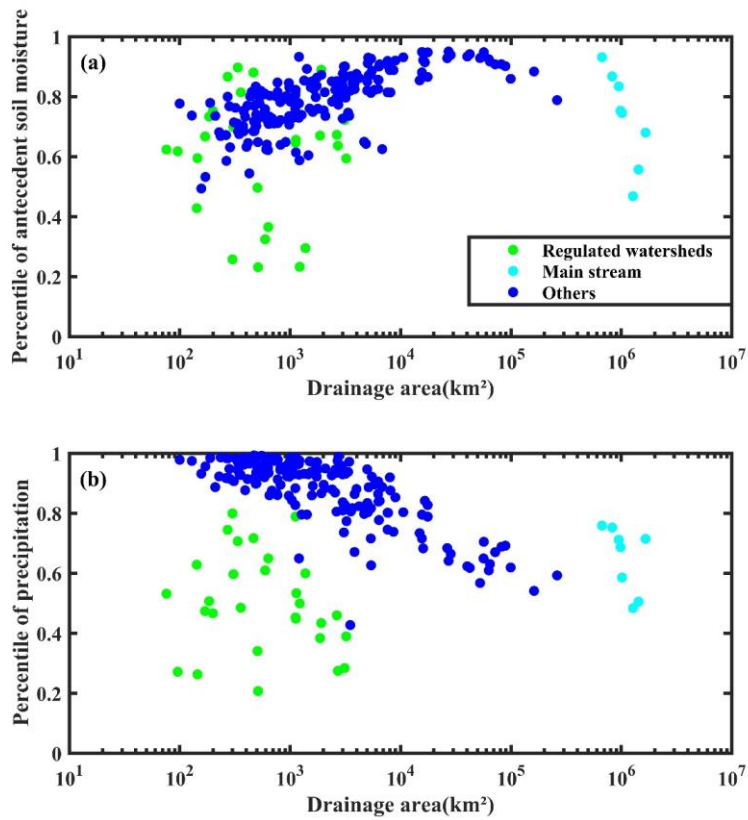
853

854 **Figure 2:** The spatial distribution of (a) the percentile of antecedent soil moisture during

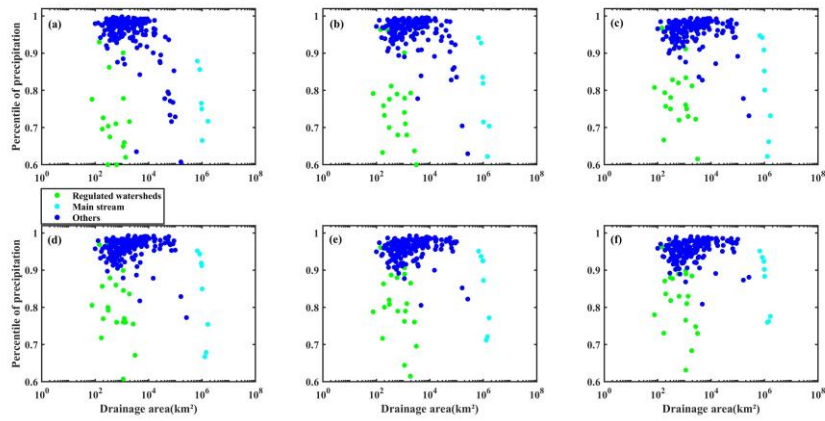
855 annual maximum flood; (b) the percentile of daily precipitation during annual

856 maximum flood.

857



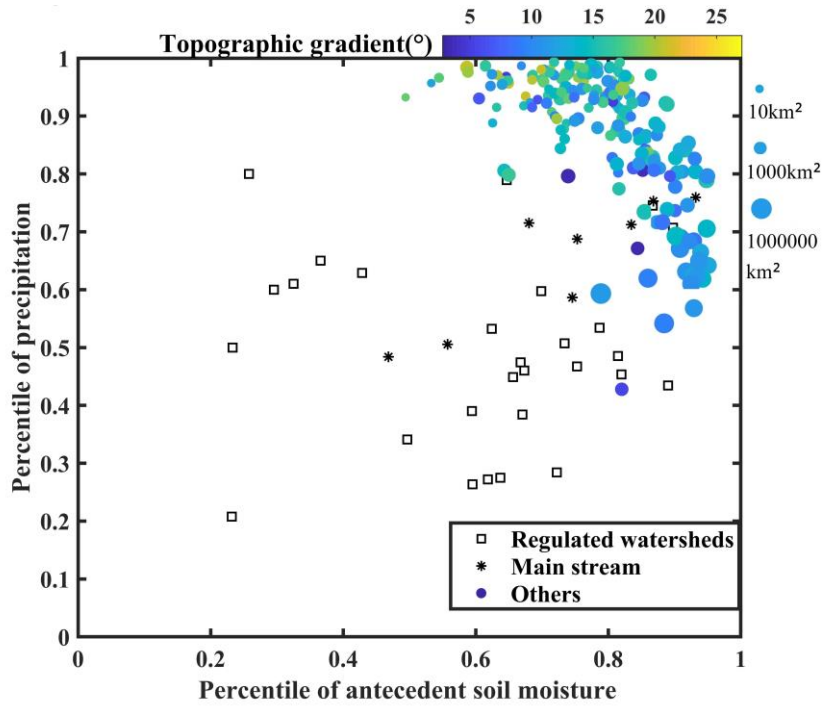
858
 859 **Figure 3:** Scatterplot between the drainage area and (a) the percentile of antecedent soil
 860 moisture of AMF events (the linear regression for blue dots: $R^2 = 0.46$, p -value<0.001);
 861 (b) the percentile of precipitation at the day of AMF events (the linear regression for
 862 blue dots: $R^2 = 0.61$, p -value<0.001). The green dots represent the regulated watershed,
 863 the cyan dots represent the sites on the main stream, and the rest sites are shown in blue.
 864
 865
 866



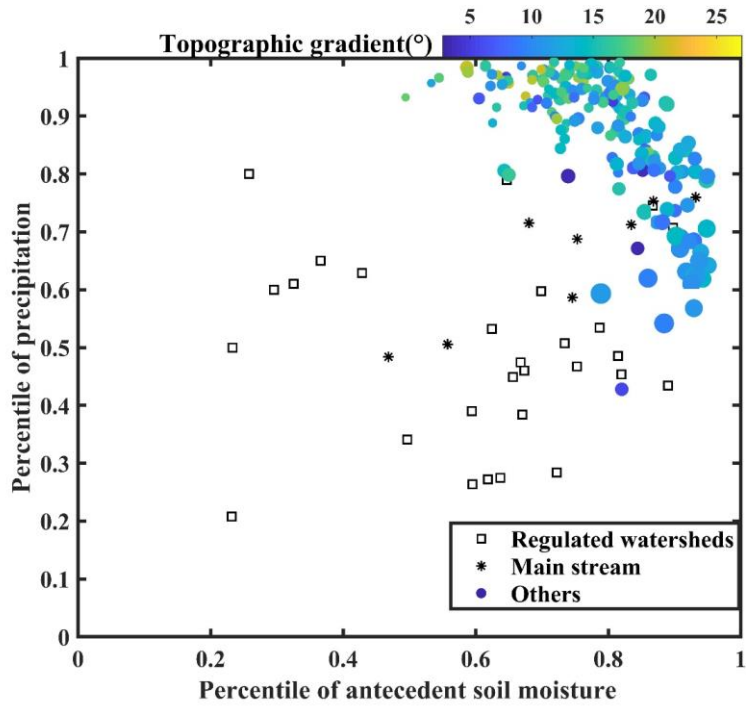
867

868 **Figure 4:** Scatterplot between the drainage area and the percentile of accumulated
 869 rainfall of (a) two days; (b) three days; (c) four days; (d) five days; (e) six days; and (f)
 870 seven days on AMF events.

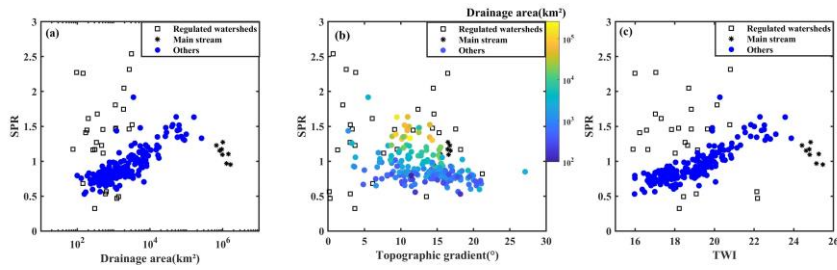
871



872



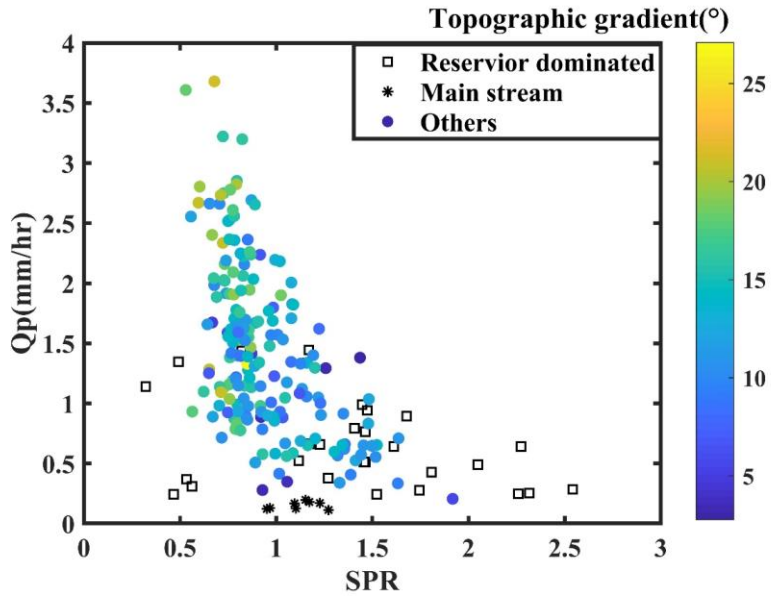
873
 874 **Figure 5:** Scatterplot of the percentile of precipitation and antecedent soil moisture, the
 875 color represents topographic gradient and the size of circles is scaled by drainage area.
 876
 877



878
 879 **Figure 6:** Scatterplots between the ratio of antecedent soil moisture and precipitation
 880 (SPR) and (a) drainage area; (b) slopetopographic gradient; and (c) topographic wetness
 881 index (TWI).

带格式的: 字体颜色: 蓝色

882



883

884 **Figure 7:** Scatterplot between the ratio of antecedent soil moisture and precipitation
885 (SPR) and area weighted annual maximum discharge (Q_p), the color represents
886 topographic gradient.

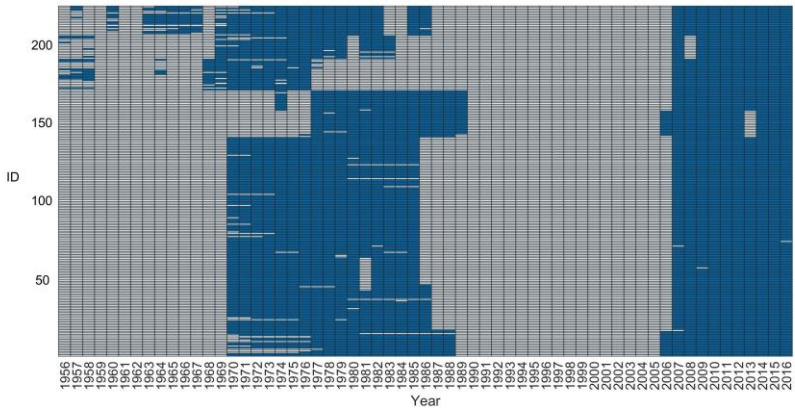
887

Supplementary

Table S1: Estimated concentration time for 10 sites with largest drainage area: the ones on main stream (MS) and the ones at the outlets of major tributaries (TR).

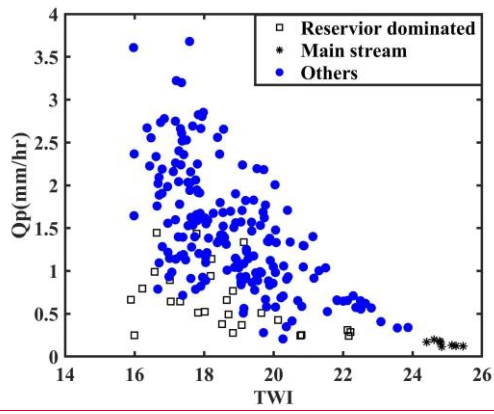
Site Name	Concentration Time (hr)	Drainage Area (km ²)
TR-Hukou	17.9	161,979
TR-Chenglingji	18.8	261,986
MS-Zhutuo	32.7	668,661
MS-Cuntan	32.8	827,799
MS-Wanxian	37.6	948,524
MS-Yichang	41.5	982,948
MS-Jianli	45.2	1,014,690
MS-Luoshan	46.3	1,276,676
MS-Hankou	51.0	1,432,008
MS-Datong	54.3	1,657,604

893
894
895
896



897
898
899
900

Figure S1: The data availability of each station, each column indicates each year while each row is corresponding to each station, blue grid indicates there is record of this year.



901

902

903

Figure S2: Scatterplot between the topographic wetness index (TWI) and area weighted annual maximum discharge (Q_p).